CHEMISTRY
A EUROPEAN JOURNAL

DOI: 10.1002/chem.200800288

Bis(guanidinate) Alkoxide Complexes of Lanthanides: Synthesis, Structures and Use in Immortal and Stereoselective Ring-Opening Polymerization of Cyclic Esters

Noureddine Ajellal,[b] Dmitrii M. Lyubov,[a] Mikhail A. Sinenkov,[a] Georgii K. Fukin,[a] Anton V. Cherkasov,[a] Christophe M. Thomas,[b] Jean-François Carpentier,*[b] and Alexander A. Trifonov*[a]

Dedicated to Professor Irina Beletskaya on the occasion of her 75th birthday

Abstract: A series of new bis(guanidinate) alkoxide Group 3 metal complexes $[Ln\{(Me_3Si)_2NC(NiPr)_2\}_2(OR)]$ (R = O*t*Bu, Ln = Y, Nd, Sm, Lu; R = O*i*Pr, Ln = Y, Nd, Lu) has been synthesized. X-ray structural determinations revealed that bis(guanidinate) *tert*-butoxides are monomeric complexes. The isopropoxide complex $[Y\{(Me_3Si)_2NC(NiPr)_2\}_2(OiPr)]$ undergoes slow decomposition in solution, to afford the unusual dimeric amido complex $[(Y\{(Me_3Si)_2NC(NiPr)_2\}_2\{\mu\text{-}N(iPr)C{\equiv}N\})_2]$. Complexes $[Ln\{(Me_3Si)_2NC(NiPr)_2\}_2(OR)]$ (R = O*t*Bu, Ln = Y, Nd, Sm, Lu; R = O*i*Pr, Ln = Y, Nd, Lu) are active catalysts/initiators for the ROP of *rac*-lactide and *rac*-β-butyrolactone under mild conditions. Most of those polymerizations proceed with a significant degree of control. Bis(guanidinate) alkoxides appear to be well suited for achieving immortal polymerization of lactide, through the introduction of large amounts of isopropanol as a chain-transfer agent. The synthesized complexes are able to promote the stereoselective ROP of *rac*-β-butyrolactone to afford syndiotactic poly(hydrobutyrate) through a chain-end control mechanism, while they are surprisingly non-stereoselective for the ROP of lactide under strictly similar conditions.

Keywords: guanidinate ligands · lactides · lanthanides · polymerization · ring-opening polymerization

Introduction

Aliphatic polyesters currently attract a growing interest as a promising alternative to synthetic petrochemical-based polymers, since the starting materials for their synthesis can be derived from annually renewable resources. Mechanical and physical properties of polyesters, together with their biodegradable and biocompatible nature, make them perspective thermoplastics with broad commercial applications (e.g., single-use packaging materials, medical sutures, and drug delivery systems).[1] Polymer properties strongly depend on intrinsic structural parameters such as polymer composition, molecular weight, polydispersity, tacticity, and polymer chain-ends.[2] Ring-opening polymerization (ROP) of cyclic esters promoted, for example, by metal initiators, proved to be the most efficient manner for preparing polyesters with controlled molecular weight and microstructure and narrow molecular-weight distribution.[3] This makes the design and synthesis of new, well-defined, single-site catalysts that exhibit good activity, productivity, and selectivity for cyclic esters polymerization and allow polymer architecture control crucial. Group 3 metals and lanthanide complexes have attracted considerable attention as initiators for the ROP of cyclic esters, and some of them have demonstrated impressive results.[4] Recently, we reported on the synthesis of lan-

[a] D. M. Lyubov, M. A. Sinenkov, Dr. G. K. Fukin, A. V. Cherkasov, Prof. Dr. A. A. Trifonov
Institute of Organometallic Chemistry
of Russian Academy of Sciences
Tropinina 49, 603950 Nizhny Novgorod GSP-445 (Russia)
Fax: (+7) 831-4627-497
E-mail: trif@iomc.ras.ru

[b] Dr. N. Ajellal, Dr. C. M. Thomas, Prof. Dr. J.-F. Carpentier
Organometallics and Catalysis, UMR CNRS 6226
Sciences Chimiques de Rennes, University of Rennes 1
35042 Rennes Cedex (France)
Fax: (+33) 223-236-939
E-mail: jcarpent@univ-rennes1.fr

Supporting information for this article is available on the WWW under http://www.chemeurj.org/ or from the author. It contains figures showing the molecular structure of complex **4a**, and ^1H and ^{13}C NMR spectra of PLAs and PHBs.

thanide borohydride complexes with bulky guanidinate ligands $[\{(Me_3Si)_2NC(NCy)_2\}_2Ln(\mu\text{-}BH_4)_2Li(thf)_2]$ (Me = methyl, Cy = cyclohexyl) that initiate the ROP of racemic lactide, providing atactic polymers with a good degree of control.[5] Since the polymerization behavior was shown to be influenced by both the ligand structure and the initiating group[6,4g] and lanthanide alkoxides proved to be efficient catalysts for ROP of cyclic esters,[4a–c,f,s,t] we focused our recent efforts on the synthesis of lanthanide alkoxides supported by guanidinate ligands. Herein we report on the synthesis and structure of complexes $[Ln\{(Me_3Si)_2NC(N\text{–}i\text{Pr})_2\}_2(OR)]$ (R = O*t*Bu, Ln = Y, Nd, Sm, Lu; R = O*i*Pr, Ln = Y, Nd, Lu) (*i*Pr = isopropyl, O*t*Bu = *tert*-butoxide, O*i*Pr = isopropoxide) and their catalytic activity in immortal and stereoselective ROP of racemic lactide and β-butyrolactone.

Results and Discussion

Synthesis and structure of bis(guanidinate) alkoxide complexes of lanthanides: Yttrium and lutetium bis(guanidinate) alkoxides $[Ln\{(Me_3Si)_2NC(N\text{–}i\text{Pr})_2\}_2(X)]$ (X = O*t*Bu, Ln = Y (**1a**), Lu (**4a**); X = O*i*Pr, Ln = Y (**1b**), Lu (**4b**)) were synthesized by metathesis reactions of the corresponding bis(guanidinate) chloro-ate-complexes $[\{(Me_3Si)_2NC(N\text{–}i\text{Pr})_2\}_2Ln(\mu\text{-}Cl)_2Li(thf)_2]$ (Ln = Y,[7] Lu[8]) with equimolar amounts of potassium *tert*-butoxide or sodium isopropoxide, respectively, in THF at room temperature (Scheme 1). For preparation of

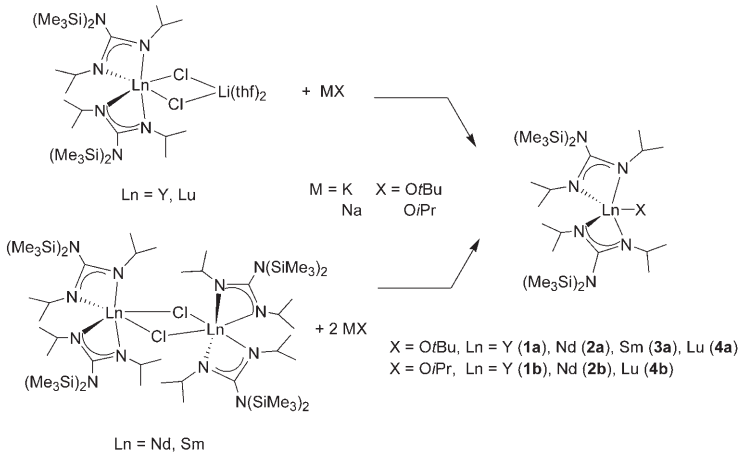

Scheme 1.

the neodymium- and samarium-containing analogues $[Ln\{(Me_3Si)_2NC(N\text{–}i\text{Pr})_2\}_2(X)]$ (X = O*t*Bu, Ln = Nd (**2a**), Sm (**3a**); X = O*i*Pr, Ln = Nd (**2b**)), dimeric bis(guanidinate) chloro complexes $[\{Ln(\mu\text{-}Cl)[(Me_3Si)_2NC(N\text{–}i\text{Pr})_2]_2\}_2]$ (Ln = Nd,[9] Sm[7]) were treated with a twofold molar excess of MX (M = K, X = O*t*Bu; M = Na, X = O*i*Pr) under similar conditions (Scheme 1). Complexes **1**–**4** were obtained after workup in high yields as oxygen and moisture sensitive solids. Complexes **1**–**4** are highly soluble in common organic solvents.

Slow concentration of solutions of *tert*-butoxide complexes **1a**–**4a** in pentane at room temperature allowed their isolation as crystalline solids. These complexes were fully characterized by elemental analysis, infrared (IR) spectroscopy, ^1H and ^{13}C NMR spectroscopy for diamagnetic complexes, and X-ray diffraction studies for **1a** and **4a**. The ^1H and $^{13}C\{^1H\}$ NMR spectra of **1a** in C_6D_6 at 20 °C show the expected sets of resonances for the guanidinate ligands and the *tert*-butoxide group. The guanidinate ligands of **1a** give in the ^1H and $^{13}C\{^1H\}$ NMR spectra a single set of signals, thus indicating equivalence of both $\{(Me_3Si)_2NC(N\textit{i}Pr)_2\}$ fragments on the NMR timescale. Complex **1a** was analyzed by X-ray crystallography. The molecular structure of **1a** is depicted in Figure 1; the crystal and structural refinement

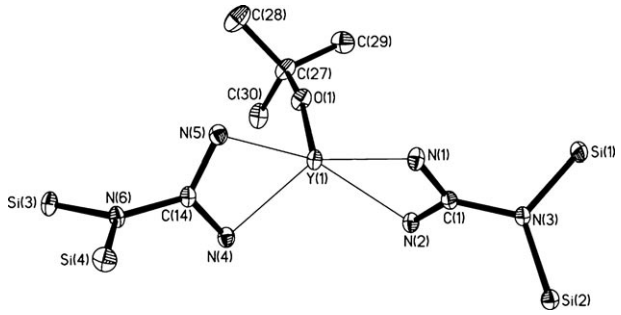

Figure 1. Molecular structure of complex **1a** with 30% probability ellipsoids; the methyl groups of $SiMe_3$ and *i*Pr fragments at N(1), N(2), N(4), N(5) are omitted for clarity. Selected distances [Å] and angles [°]: Y(1)–O(1) 2.021(2), Y(1)–N(1) 2.340(2), Y(1)–N(2) 2.367(3), Y(1)–N(4) 2.325(3), Y(1)–N(5) 2.374(2), N(1)–C(1) 1.328(4), C(1)–N(2) 1.333(4), N(4)–C(14) 1.335(4), N(4)–C(15) 1.459(4), N(5)–C(14) 1.331(4), O(1)-Y(1)-N(1) 123.52(9), O(1)-Y(1)-N(2) 106.17(9), O(1)-Y(1)-N(4) 115.38(9), N(4)-Y(1)-N(1) 121.09(9), N(4)-Y(1)-N(2) 107.30(9), N(1)-Y(1)-N(2) 56.85(9), O(1)-Y(1)-N(5) 104.58(9), N(4)-Y(1)-N(5) 57.31(9), N(1)-Y(1)-N(5) 105.56(9).

data are listed in Table 1. Complex **1a** is a monomeric THF-free compound in the solid state. The coordination sphere of the yttrium atom is made up of the four nitrogen atoms of the two chelating guanidinate ligands and the oxygen atom of the O*t*Bu group, thus resulting in a formal coordination number of five. The Y–N bond lengths in **1a** are very similar (2.325(3)–2.374(2) Å) and are comparable to those reported for related bis(guanidinate)–yttrium complexes.[10] The N–C bond lengths in the guanidinate ligands differ only slightly from each other (1.328(4)–1.335(4) Å), reflecting electron delocalization within the anionic NCN units. These features are consistent with the symmetry observed in solution by NMR spectroscopy. The Y–O bond length in **1a** of 2.021(2) Å compares well with the value of 2.005(10) Å found for terminal Y–O distances in the six-coordinate yttrium complex $[\{YCp(\mu\text{-}OCMe_3)(OCMe_3)\}_2]$ (Cp = cyclopentadienyl).[11]

A single-crystal X-ray diffraction study for the lutetium analogue **4a** revealed its structural similarity to **1a** (see Supporting Information; Figure S1). Unlike complex **1a**, the bonding situations within the two metallacyclic fragments

Table 1. Crystallographic data and structure refinement details for **1a**, **4a** and **1c**.

	1a	**4a**	**1c**
formula	$C_{30}H_{73}N_6OSi_4Y$	$C_{30}H_{73}LuN_6OSi_4$	$C_{60}H_{142}N_{16}Si_8Y_2$
M_r	735.21	831.72	1490.44
T [K]	100(2)	100(2)	100(2)
λ [Å]	0.71073	0.71073	0.71073
crystal system	monoclinic	monoclinic	monoclinic
space group	$C2/c$	$C2/c$	$P2_1/n$
a [A]	33.5255(18)	33.660(8)	15.1587(4)
b [A]	15.5956(8)	15.539(4)	11.9779(3)
c [A]	18.3564(10)	18.305(4)	22.9861(7)
α [°]	90	90	90
β [°]	114.6540(10)	114.661(4)	92.9440(10)
γ [°]	90	90	90
V [Å^3]	8722.8(8)	8701(3)	4168.1(2)
Z	8	8	2
ρ_{calcd} [g cm^{-3}]	1.120	1.254	1.188
μ [mm^{-1}]	1.475	2.407	1.544
F(000)	3184	3440	1608
crystal size [mm^3]	0.40×0.35× 0.30	0.21×0.16×0.03	0.34×0.31×0.23
θ range [°]	1.34–26.00	1.73–26.00	2.37–27.50
index ranges	$-41 \le h \le 41$	$-41 \le h \le 41$	$-19 \le h \le 19$
	$-19 \le k \le 19$	$-19 \le k \le 19$	$-15 \le k \le 15$
	$-22 \le l \le 22$	$-22 \le l \le 22$	$-29 \le l \le 29$
reflns collected	36736	35158	39454
independent reflns	8584[$R(int)$ = 0.0449]	8540 [$R(int)$ = 0.0732]	9550 [$R(int)$ = 0.0336]
completeness to θ	99.9	99.6	99.7
data/restraints/parameters	8584/16/397	8540/23/398	9550/9/672
goodness-of-fit on F^2	1.180	1.213	1.027
final R indices [$I > 2\sigma(I)$]	$R1$ = 0.0480	$R1$ = 0.0640	$R1$ = 0.0294
	$wR2$ = 0.1026	$wR2$ = 0.1331	$wR2$ = 0.0652
R indices (all data)	$R1$ = 0.0599	$R1$ = 0.0763	$R1$ = 0.0442
	$wR2$ = 0.1056	$wR2$ = 0.1361	$wR2$ = 0.0693
largest diff. peak/hole [e Å^{-3}]	0.755/−0.602	2.197/−4.191	0.502/−0.202

LuNCN in **4a** differ noticeably. The two Lu–N bond lengths for one guanidinate ligand are slightly different (2.294(4) and 2.323(4) Å), while for the second ligand, the nonequivalence of these bonds is more pronounced (2.269(5) and 2.331(4) Å). A substantial difference in the N–C bonds within the NCN fragments is also observed: 1.334(6) and 1.339(6) Å for the first ligand versus 1.314(7) and 1.356(6) Å for the second. Evidently, the small value of the ionic radius of lutetium leads to a slightly unsymmetrical coordination of the guanidinate ligands.[12]

The asymmetric coordination of the guanidinate ligands in **4a** is also evident in solution as shown by ^{1}H and ^{13}C{^{1}H} NMR spectroscopy. The nonequivalent $SiMe_3$ groups appear in the ^{1}H NMR spectrum as a set of three singlets at δ = 0.14, 0.24, and 0.33 ppm, and the methyl groups of the isopropyl fragments also give rise to three doublets at δ = 1.00, 1.23, and 1.27 ppm ($^3J_{H\text{-}H}$ = 6.2 Hz); accordingly, three septets ($^1J_{H\text{-}H}$ = 6.2 Hz) at δ = 3.75, 3.89, and 4.04 ppm are found for the CH hydrogen atoms of the isopropyl groups. Moreover, the *tert*-butoxide group appears as two singlets at δ = 1.43 and 1.52 ppm with a 2:1 integral ratio, thus reflecting hindered rotation of this moiety. Similarly, the ^{13}C{^{1}H} NMR spectrum of **4a** contains three signals for $SiMe_3$ groups (δ = 1.6, 2.1, 2.3 ppm) and three signals for both the methyl and methine carbons of the isopropyl fragments (δ = 22.6, 22.8, 26.8 ppm and 42.5, 45.7, 47.7 ppm, respectively). Also, the methyl carbons of the *tert*-butoxide group give rise to two signals (δ = 31.6, 34.7 ppm).

Isopropoxide complexes **1b**–**4b** were isolated in high yields (90–93%) following analogous procedures and fully characterized by elemental analysis, IR spectroscopy, and ^{1}H and ^{13}C NMR spectroscopy for diamagnetic complexes. Slow evaporation of solutions of the complexes in hexane under vacuum afforded amorphous powders. Unfortunately, all our attempts to obtain crystalline samples of **1b**–**4b** suitable for X-ray diffraction studies have failed so far.

To our surprise, we have found that bis(guanidinate) *tert*-butoxide and isopropoxide complexes feature remarkably different stabilities. Thus, *tert*-butoxides **1a**–**4a** are stable in both the solid state and hexane or benzene, since no changes have been observed in their ^{1}H NMR (**1a**, **4a**) and IR spectra (**1a**–**4a**) when stored for a long time (over several months) at room temperature. However, isopropoxides **1b**–**4b** are rather unstable and slowly decompose. For example, prolonged storage (two months) at room temperature of a concentrated hexane solution of **1b** afforded crystals of the unexpected complex [(Y{(Me$_3$Si)$_2$NC(N*i*Pr)$_2$}$_2${μ-N(*i*Pr)C≡N})$_2$] (**1c**).[13] Apparently, this species results from the cleavage of two C–N bonds of the guanidinate ligand (Scheme 2). Another type of fragmentation of guanidinate ligands, which includes a 1,3-shift of the Me_3Si group and C–N bond cleavage and which resulted in the formation of the mixed ligand

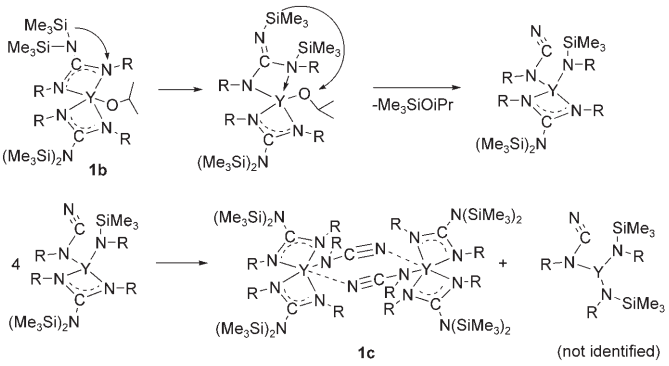

Scheme 2. Possible mechanistic pathway for the degradation of **1b** into **1c**.

guanidinate amido calcium complex $[(Ca\{(Me_3Si)_2NC(NCy)_2\}\{\mu\text{-}(Me_3Si)(Cy)N\})_2]$, has been previously reported.[14]

Complex **1c** was characterized by X-ray crystallography, but all the attempts to obtain this compound in an analytically pure form failed due to the presence of a second microcrystalline byproduct, which we were unable to separate by recrystallization. The molecular structure of **1c** is depicted in Figure 2; crystal and structural refinement data are

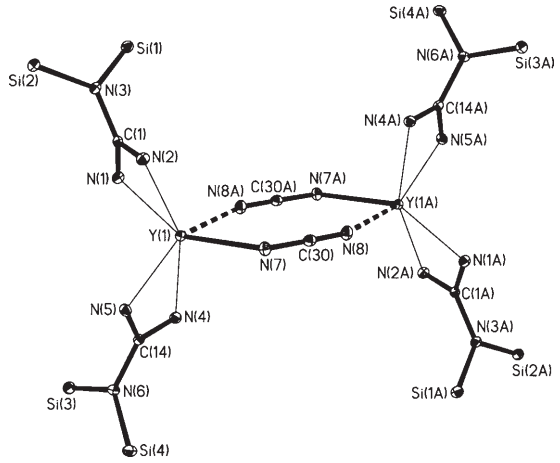

Figure 2. Molecular structure of complex **1c** with 30% probability ellipsoids; the methyl groups of $SiMe_3$ and *i*Pr fragments at N(1), N(2), N(4), N(5), N(7), N(1A), N(2A), N(4A), N(5A), N(7A) are omitted for clarity. Selected distances [Å] and angles [°]: Y(1)–N(1) 2.3440(9), Y(1)–N(2) 2.3922(9), Y(1)–N(4) 2.3654(9), Y(1)–N(5) 2.3796(9), Y(1)–N(7) 2.4251(9), Y(1)–N(8 A) 2.359(1), N(8)–Y(1 A) 2.359(1), N(1)–C(1) 1.334(1), N(2)–C(1) 1.336(1), N(4)–C(14) 1.333(1), N(5)–C(14) 1.330(1), N(7)–C(30) 1.299(2), N(7)–C(27) 1.499(1), N(8)–C(30) 1.163(2), N(8 A)-Y(1)-N(7) 80.69(3), N(1)-Y(1)-N(2) 56.20(3), N(4)-Y(1)-N(5) 56.34(3), N(8)-C(30)-N(7) 177.0(1), C(30)-N(7)-C(27) 114.37(9).

listed in Table 1. In the solid state, complex **1c** is a dimer in which two $\{Y\{(Me_3Si)_2NC(N\mathit{i}Pr)_2\}_2\}$ moieties are linked by the two μ-bridging $\{N(\mathit{i}Pr)C{\equiv}N\}$ fragments. The coordination sphere of the yttrium atom is made up of four nitrogen atoms of the two bidentate guanidinate ligands and two nitrogen atoms of the two μ-bridging $\{N(\mathit{i}Pr)C{\equiv}N\}$ fragments. This results in a formal coordination number of six. The Y–N(guanidinate) bond length are similar (2.3440(9)–2.3922(9) Å) and comparable to the distances reported for related bis(guanidinate)–yttrium complexes.[10] On the other hand, the Y–N(amido) bond length (2.425(9) Å) is notably longer than related bond lengths in seven-coordinate metallocene-type yttrium–amido complexes (2.254(1)–2.281(5) Å)[15] and the five-coordinate bis(guanidinate)amido complex $[Y\{(Me_3Si)_2NC(N\mathit{i}Pr)_2\}_2\{N(\mathit{i}Pr)_2\}]$ (2.199(3) Å).[9] Surprisingly, this covalent Y–N bond is even longer than the bond between the same yttrium atom and the nitrogen atom of the cyano group (2.359(1) Å); this lengthening of the bond evidently caused by steric hindrance. It is worth pointing out the unusual bonding situation within the bridging N(*i*Pr)C≡N ligand. There are three different C–N bonds in this fragment. The first bond (C(30)–N(8)) is very short (1.162(2) Å) and can be considered as a triple C≡N bond.[16] The presence of C≡N bonds in complex **1c** is confirmed by its IR spectrum, which contains a strong absorption band at $\tilde{\nu}=2141\ cm^{-1}$. The N(7)–C(30) bond, which should in fact be a single bond, was found to be noticeably shorter (1.299(2) Å) than expected for a single C–N bond and its length can be attributed to a double C=N bond.[15] Apparently, this C–N bond contraction results from the p–π conjugation between the π-electrons of the triple C≡N-bond and the p electrons of the lone electron pair of the nitrogen atom.

The bis(guanidinate)isopropoxide–neodymium complex **2b** also undergoes slow decomposition, as indicated by the appearance of the strong absorption band at $\tilde{\nu}=2118\ cm^{-1}$ in its IR spectrum.

Ring-opening polymerization of racemic lactide: The prepared complexes **1–4** were first evaluated in the ROP of *rac*-lactide (Scheme 3). Representative results are summarized

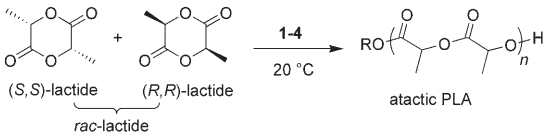

Scheme 3.

in Table 2. All complexes proved to be active under mild conditions, allowing full conversion of 100–500 equivalents of lactide (LA) in 1–14 h (reaction times not optimized) at 20 °C in either toluene or THF at $[rac\text{-LA}]=1.0\ mol\,L^{-1}$. No

Table 2. Ring-opening polymerization of *rac*-lactide with complexes **1–4a,b**.[a]

	Complex	[LA]/[Ln]	Solvent	*t* [h][b]	Yield [%][c]	$M_{n,calcd}$[d] ($\times10^3$)	$M_{n,exptl}$[e] ($\times10^3$)	M_w/M_n[e]
1	**1a**	100	THF	14	55	7.9	7.7	1.22
2	**1a**	100	Tol	14	93	13.4	9.3	1.64
3	**1b**	100	THF	3	98	14.1	9.7	1.50
4	**1b**	100	Tol	20	51	7.3	6.4	1.12
5	**2a**	100	THF	14	95	13.7	14.8	1.62
6	**2a**	100	Tol	14	94	13.5	19.7	1.56
7	**2a**	500	Tol	14	97	69.8	54.2	1.77
8	**2b**	100	THF	1	96	14.4	8.0	1.42
9[f]	**2b**	1000	THF	20	41	59.0	26.0	1.50
10	**2b**	100	Tol	3	95	13.7	8.0	1.44
11	**2b**	200	Tol	6	90	26.0	16.9	1.40
12	**3a**	100	Tol	14	94	13.5	7.0	1.72
13	**4a**	100	THF	14	44	6.3	8.7	1.23
14	**4a**	100	Tol	14	85	12.3	13.3	1.59
15	**4b**	100	Tol	14	77	11.1	5.3	1.27

[a] All reactions were performed with $[rac\text{-LA}]=1.0\ M$ at 20 °C, unless otherwise stated; results are representative of at least duplicated experiments. [b] Reaction times were not necessarily optimized. [c] Isolated yields of PLA. [d] M_n (in $g\,mol^{-1}$) of PLA calculated from $M_{n,calcd}=144.00\times([LA]/[Ln])\times$ yield(LA). [e] Experimental (corrected; see Experimental section) M_n (in $g\,mol^{-1}$) and M_w/M_n values determined by GPC in THF against polystyrene standards. [f] $[rac\text{-LA}]=3.0\ M$.

evident differences in the behavior of *tert*-butoxide and isopropoxide complexes could be discerned in these ROP reactions. On the other hand, the polymerization activities and, to a lesser extent, the overall control over the molecular weights (i.e., agreement of experimental with calculated M_n values, and molecular weight distributions) are significantly affected by the nature of the metal center. The polymerization solvent appeared to play a significant role as well. Thus, *tert*-butoxide complexes **1a** and **4a**, which both contain a small metal center (Y and Lu, respectively),[12] showed very similar performances (compare entries 1 and 2 with 13 and 14 in Table 2). In particular, those systems feature higher activity in toluene than in THF. This observation follows the usual trend in the ROP of lactide, completion times are shorter in apolar, non-coordinating solvents, such as toluene, than in THF;[4i,j] this common fact has been tentatively rationalized by the high affinity of oxophilic metals such as lanthanides for THF, which could result in a competition with the lactide monomer in the coordination at the metal center. On the other hand, an opposite trend was observed for the isopropoxide complex **1b**; the ROP of LA proceeds significantly faster in THF than in toluene (entries 3 and 4 in Table 2), which is observed much more seldom.[4h] The *tert*-butoxide and isopropoxide complexes **2a**,**b** that have a larger neodymium center do not show such significant solvent dependence on ROP activities (entries 5–9 in Table 2). For the series of reactions carried out in THF, both with the *tert*-butoxide complexes **1a**–**4a** and isopropoxide complexes **1b** and **2b**, the observed decreasing order of activity was $Nd \approx Sm > Y \approx Lu$, suggesting an apparent correlation with ionic radii of the lanthanide centers.[12]

All the polylactides (PLAs) obtained with complexes **1**–**4** showed monomodal gel-permeation chromatography (GPC) traces with relatively narrow molecular weight distributions ($1.12 < M_w/M_n < 1.77$), indicative of a single-site character (see below). The number average molecular mass (M_n) values increase with the monomer-to-metal ratio (entries 6/7, and 10/11 in Table 2), though not always linearly (entries 8/9). The corrected experimental M_n values of the PLAs produced with those complexes are, in most cases, close to the theoretical ones, calculated on the assumption that a single PLA chain is produced per metal center through initiation of the polymerization by the alkoxide group.

To explore the possibility of achieving immortal polymerization with these systems, that is, to generate several PLA chains per metal center by introducing several equivalents of a chain-transfer agent, experiments were conducted in the presence of isopropanol.[17] Complex **2a**, which showed good matching of experimental and calculated M_n values, that is, high initiation efficiency, and the ability to convert at least up to 500 equiv of lactide (Table 2, entry 7), was selected for this purpose. Representative results are summarized in Table 3. The **2a**/*i*PrOH system proved able to quantitatively convert 500 equivalents of lactide with up to 50 equivalents of chain-transfer agent per metal initiator. All the obtained PLAs showed monomodal, relatively narrow distributions with an excellent correlation between the experimental and calculated M_n values (entries 2–7 in Table 3). These observations establish that 1) the metal complex is stable in the presence of large amounts of free alcohol (i.e. the guanidinate ligands are not displaced), and 2) a fast reversible exchange between free alcohol and growing PLA chains takes place during the polymerization process (Scheme 4). High productivities (up to 1600 mol(LA) mol(Nd)$^{-1}$) could be achieved by increasing the monomer to initiator ratio to 2000, while still using 50 equivalents of chain-transfer agent (entries 7 and 8 in Table 3). Poor conversion was observed when using a very large amount of lactide (5000 equiv relative to **2a**, entry 9 in Table 3) and is likely due to the difficulty of sufficiently purifying lactide and avoiding poisoning at such a low catalyst loadings. Nevertheless, to our knowledge, these performances in terms of productivity and chain-transfer efficiency are among the best reported thus far for the ROP of lactide with metal-based initiators.[17]

Table 3. Immortal ring-opening polymerization of *rac*-lactide in the presence of **2a**/isopropanol systems.[a]

	[*i*PrOH]/[**2a**]	[LA]/[**2a**]	*t* [h][b]	Yield [%][c]	$M_{n,calcd}$[d] ($\times 10^3$)	$M_{n,exptl}$[e] ($\times 10^3$)	M_w/M_n[e]
1	0	500	14	97	69.8	54.2	1.77
2	3	500	14	97	23.2	20.6	1.46
3	5	500	14	98	14.1	12.7	1.59
4	10	500	14	98	7.1	7.5	1.62
5	20	500	14	96	3.5	5.3	1.20
6	50	500	14	98	1.4	1.9	1.24
7[f]	50	1000	18	98	2.9	4.8	1.18
8[f]	50	2000	26	79	4.6	6.0	1.14
9[f]	50	5000	26	<5	n.d.[g]	n.d.	n.d.

[a] All reactions were performed with [*rac*-LA] = 1.0 M in toluene at 20 °C, unless otherwise stated. [b] Reaction times were not optimized. [c] Isolated yields of PLA. [d] M_n (in g mol^{-1}) of PLA calculated from $M_{n,calcd} = 144.00 \times ([LA]/[Ln]) \times$ yield(LA). [e] Experimental (corrected; see Experimental section) M_n (in g mol^{-1}) and M_w/M_n values determined by GPC in THF against polystyrene standards. [f] [*rac*-LA] = 3.0 M. [g] n.d. = not determined.

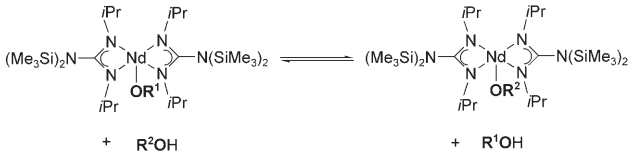

Scheme 4. R^1,R^2 = first initiating group and free alcohol, then growing PLA chains.

All the PLAs produced from *rac*-lactide with complexes **1**–**4** show atactic microstructures as determined by NMR analysis (see Supporting Information; Figure S2).[18] A control polymerization of (*S*,*S*)-lactide by **2a** in toluene resulted in pure isotactic PLA, evidenced by the observation of a single sharp resonance for the methine region in the decoupled ^{1}H NMR spectrum. This observation supports the lack of base promoted epimerization of lactide or PLA (which may transform an initially stereo-enriched polymer into an

atactic one) and argues against an anionic polymerization mechanism.[19,20]

Ring-opening polymerization of racemic β-butyrolactone: Surprisingly, although not stereoselective for the polymerization of *rac*-lactide, complexes **1–4** proved able to control the stereoselective ROP of β-butyrolactone (BBL) to produce syndiotactic rich poly(hydroxy-3-butyrate) (PHB) (Scheme 5). Previous studies have shown that the ROP of

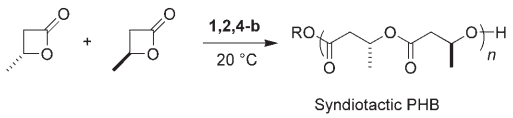

Scheme 5.

BBL is generally much more difficult than that of lactide,[21] and very few metal-based initiators have been shown to induce high stereoselectivities.[4j] For instance, zinc–imidinate complexes introduced by Coates, which produce highly heterotactic PLA from *rac*-lactide,[22] lead to purely atactic PHB from *rac*-BBL.[23]

The results summarized in Table 4 reveal first that the neodymium–isopropoxide complex **2b** allowed turnover numbers (TONs) up to 200 within a few hours at 20 °C in toluene (entries 1 and 2 in Table 4). However, the PHBs recovered under those conditions were all atactic (see Supporting Information; Figure S3). Keeping in mind that the stereoselectivity of ROP reactions is often inversely related to the ionic radius of metal centers, as we demonstrated in the ROP of *rac*-lactide with aminoalkoxybis(phenolate) Group 3 metal complexes,[4i] we next focused on isopropoxide complexes bearing smaller metal centers. In fact, ROP of *rac*-BBL promoted by yttrium and lutetium complexes **1b** and **4b**, respectively, offered syndiotactic enriched PHB, with a probability of racemic linkages between monomer units (P_r) up to 84% (entries 3–6 and 10 in Table 4). The P_r value in PHBs is readily determined from both the methyl and carbonyl regions of the ^{13}C NMR spectrum, which feature well resolved resonances for the *racemic* (*r*) and *meso* (*m*) diad sequences (Figure 3).[4j,24]

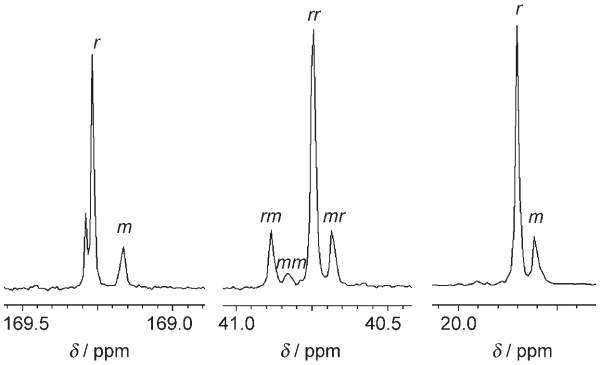

Figure 3. Carbonyl, methylene, and methyl regions of the $^{13}C\{^1H\}$ NMR spectrum (125 MHz, $CDCl_3$, 20 °C) of a syndiotactic rich ($P_r = 0.84$) PHB sample prepared by polymerization of *rac*-BBL in THF with complex **1b** (Table 4, entry 3).

The yttrium complex proved much more active than its lutetium congener and further investigations were therefore conducted with the former complex. Complex **1b** offered quite similar results in THF and toluene in terms of activity, stereoselectivity, and control over the molecular weights (compare entries 3 and 4 in Table 4). Much poorer results were obtained by using dichloromethane and hexane as the solvent (entries 8 and 9 in Table 4). In particular, the stereocontrol achieved with **1b** in the latter solvents ($P_r = 0.54$–0.60) was nearly as poor as that achieved in toluene with the simple homoleptic initiators [Y{N(SiHMe$_2$)$_3$}$_3$] and "[Y(O*i*Pr)$_3$]" (generated in situ) ($P_r = 0.55$ and 0.51, respectively).[4j]

Detailed microstructural analysis by ^{13}C NMR spectroscopy confirmed a chain-end control mechanism. The methylene region of the $^{13}C\{^1H\}$ NMR spectrum of the PHBs produced with **1b** and **2b** contains an intense resonance at $\delta = 40.69$ ppm assigned to the *rr* triad (*r* = racemic diad), two resonances of equal, intermediate intensity at $\delta = 40.63$ and 40.83 ppm for the *mr* (*m* = *meso* diad) and the *rm* triads, and a fourth very weak resonance at $\delta = 40.85$ ppm for the *mm* triad (Figure 3). The

Table 4. Ring-opening polymerization of *rac*-β-butyrolactone with complexes **1–4b**.[a]

	Complex	[BBL] [mol L^{-1}]	[BBL]/[Ln]	Solvent	*t* [h]	conv. [%][b]	$M_{n,calcd}$[c] ($\times 10^3$)	$M_{n,exptl}$[d] ($\times 10^3$)	M_w/M_n[d]	P_r[e]
1	**2b**	3	100	Tol	2	96	8.3	8.1	1.09	0.45
2	**2b**	3	400	Tol	8	51	17.5	25.8	1.48	0.45
3	**1b**	3	100	THF	2	95	8.2	15.2	1.22	0.84
4	**1b**	3	100	Tol	2	93	8.0	14.6	1.18	0.80
5	**1b**	3	200	Tol	5	72	12.4	17.8	1.21	0.80
6	**1b**	6	400	Tol	8	60	20.6	28.2	1.27	0.80
7[f]	**1b**	6	400	Tol	8	26	3.0	2.5	1.13	n.d.
8	**1b**	3	100	CH_2Cl_2	6	70	6.0	3.4	1.22	0.54
9	**1b**	3	100	Hex	6	54	4.7	2.0	1.69	0.60
10	**4b**	3	100	Tol	14	27	2.3	2.7	1.34	0.82

[a] All reactions performed at 20 °C, unless otherwise stated. [b] Conversion of *rac*-BBL as determined by the integration of ^1H NMR methine resonances of *rac*-BBL and PHB; isolated yields of PHB were essentially similar ±5%, except for low molecular weight polymers which are difficult to precipitate. [c] M_n (in g mol^{-1}) of PHB calculated from $M_{n,calc} = 86.00 \times ([BBL]/[Ln + i\text{PrOH}]) \times$ conversion BBL. [d] Experimental (uncorrected) M_n (in g mol^{-1}) and M_w/M_n values determined by GPC in THF against polystyrene standards. [e] P_r is the probability of racemic linkages between β-butyrolactone units and is determined by $^{13}C\{^1H\}$ NMR spectroscopy. [f] 3 equiv of *i*PrOH added against Ln.

relative intensities of these four resonances for a PHB produced from **1b** in toluene (Table 4, entry 4) are 0.70:0.14:0.12:0.04, which fit the calculated values well for a Bernoullian statistics with $P_r = 0.84$: $(rr) = (P_r)^2 = 0.705$, $(rm) = (mr) = (P_r)(1 - P_r) = 0.13$, and $(mm) = (1 - P_r)^2 = 0.03$.

All the PHBs obtained with complexes **1b**, **2b**, and **4b** in toluene or in THF showed unimodal GPC traces with relatively narrow molecular weight distributions ($1.09 < M_w/M_n < 1.48$), indicative of a single-site character, as above mentioned for the ROP of *rac*-lactide (see below).[25] Also, the experimental M_n values increase with the monomer conversion (entries 1, 2, and 4–6 in Table 4) and are close to the theoretical ones, calculated on the assumption that a single PHB chain is produced per metal center by initiation of the polymerization by the alkoxide (isopropoxide) group. This assumption was further demonstrated by NMR spectroscopy. The ^{1}H NMR spectra in $CDCl_3$ of relatively low molecular-weight samples of PHB show the (broadened) quartet characteristic of the C*H*(Me)OH terminal group at $\delta =$ 4.33 ppm (Figure 4). This group is formed after hydrolysis of

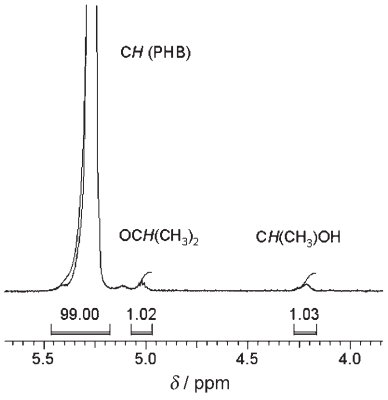

Figure 4. Detail of the ^{1}H NMR spectrum (500 MHz, $CDCl_3$, 20 °C) showing the resonances assigned to the terminal groups of the polymer chain in a PHB sample prepared by polymerization of *rac*-BBL in toluene with isopropoxide complex **2b** (Table 4, entry 1).

the metal–alkoxide bond, an observation which is indicative of a classical coordination/insertion mechanism with an initial ring opening through acyl–oxygen bond cleavage.[26] The observation of another quartet resonance of equal intensity at $\delta = 5.02$ ppm establishes the presence of an isopropoxycarbonyl function at the other extremity of the PHB chain (Figure 4). This assignment, also supported by ^{13}C NMR spectroscopy (see Supporting Information; Figure S4), confirms that the isopropoxide (alkoxide) ligand in this series of complexes is the true initiator of the ROP process.

Conclusion

We have prepared and structurally characterized both in solution and in the solid state a variety of new bis(guanidinate) alkoxide Group 3 metal complexes. This series of complexes allowed a direct comparison of the ubiquitous isopropoxide and much more seldom used *tert*-butoxide as potential initiating groups for the ROP of cyclic esters. In fact, all those complexes have been shown to be active for the ROP of *rac*-lactide and *rac*-β-butyrolactone under mild conditions. Most of those polymerizations proceed with a significant degree of control, offering PLAs and PHBs with relatively narrow molecular weight distributions and experimental M_n values in close agreement with the calculated ones. Interestingly, this class of bis(guanidinate) initiators appears to be well suited for achieving immortal polymerization of lactide through the introduction of large amounts of isopropanol as a chain transfer agent, thus enabling the conversion of large amounts of monomer and the production of many macromolecular chains per metal initiator. Probably the most interesting observation in this work is the demonstrated capability of metal complexes to promote the stereoselective ROP of *rac*-β-butyrolactone through a chain-end control mechanism, while those complexes are essentially non-stereoselective for the ROP of lactide under strictly similar conditions. This unexpected observation, which is unprecedented to our knowledge, demonstrates that, despite the close similarities usually anticipated in the ROP of lactide and β-butyrolactone, (still) subtle parameters can significantly affect the final outcome. Efforts are in progress in our laboratories to expand on this family of bis(guanidinate) alkoxide complexes to further improve their catalytic performances.

Experimental Section

General conditions: All manipulations requiring an anhydrous atmosphere were performed under a purified argon atmosphere using standard Schlenk techniques or in a glove box. *N,N′*-Diisopropylcarbodiimide was purchased from Acros, dried with molecular sieves and purified by condensation in vacuum. Anhydrous $LnCl_3$[27] and $[Li\{N(SiMe_3)_2\}(Et_2O)]$[28] were prepared according to literature procedures. Solvents (toluene, THF, hexane) were freshly distilled from Na/K alloy under nitrogen and degassed thoroughly by freeze–pump–thaw cycles prior to use. CH_2Cl_2 was dried over CaH_2, distilled twice, and degassed by freeze–pump–thaw cycles prior to use. Deuterated solvents, except $CDCl_3$, were freshly distilled from Na/K amalgam under argon and degassed prior to use. Racemic lactide (Aldrich) was recrystallized twice from dry toluene and then sublimed under vacuum at 50 °C. Racemic β-butyrolactone (Aldrich) was freshly distilled from CaH_2 under nitrogen and degassed thoroughly by freeze pump thaw cycles prior to use.

Instruments and measurements: IR spectra were recorded as Nujol mulls on a FSM 1201 spectrophotometer. NMR spectra were recorded on Bruker AM-500 and DPX-200 spectrometers in C_6D_6 or $CDCl_3$ at 20 °C, unless otherwise stated. C and H elemental analyses were performed by the microanalytical laboratory of IOMC. Lanthanide metal analysis was carried out by complexometric titration. Size-exclusion chromatography (SEC) of PLAs and PHBs was performed in THF at 20 °C using a Polymer Laboratories PL50 apparatus equipped with PLgel 5 μm MIXED-C 300 × 7.5 mm columns, and combined RI and Dual angle LS (PL-LS 45/90°) detectors. The number average molecular masses (M_n) and polydispersity index (M_w/M_n) of the polymers were calculated with reference to a universal calibration against polystyrene standards. M_n values of PLAs were corrected with a Mark–Houwink factor of 0.58 to account for the difference in hydrodynamic volumes between polystyrene and polylactide.[29] The microstructure of PLAs was determined by homodecoupling

^{1}H NMR spectroscopy at 20 °C in $CDCl_3$ with a Bruker AC-500 spectrometer.[18] The microstructure of PHBs was determined by analyzing the carbonyl region of $^{13}C\{^1H\}$ NMR spectra at 20 °C in $CDCl_3$ with a Bruker AC-500 spectrometer operating at 125 MHz (see text for details).[4b]

Synthesis of bis(guanidinate) alkoxide complexes of lanthanides

*[Y{(Me$_3$Si)$_2$NC(N-iPr)$_2$}$_2$(OtBu)] (**1a**)*: A solution of KO*t*Bu (0.17 g, 1.50 mmol) in THF (10 mL) was added to a solution of [{(Me$_3$Si)$_2$NC(N*i*Pr)$_2$}$_2$Y(μ-Cl)Li(thf)$_2$] (1.19 g, 1.35 mmol) in THF (40 mL) at room temperature, and the reaction mixture was stirred for 24 h. The solution was filtered and the solvent was evaporated in vacuo. The off-white solid residue was extracted with toluene (20 mL), and the extract was filtered. Evaporation of toluene in vacuo and recrystallization of the resulting solid from pentane afforded colorless crystals of **1a** (0.73 g, 74 %). ^{1}H NMR (200 MHz, [D$_6$]benzene): δ = 0.19, 0.29 (2 s, together 36 H; NSi(CH_3)$_3$), 1.31 (d, $^3J_{H\text{-}H}$ = 6.2 Hz, 24 H; CH(CH_3)$_2$), 1.46 (s, 9 H; *t*Bu), 3.79 ppm (sept, $^3J_{H\text{-}H}$ = 6.2 Hz, 4 H; C*H*(CH$_3$)$_2$); $^{13}C\{^1H\}$ NMR (50 MHz, [D$_6$]benzene): δ = 2.2 (N(Si*C*H$_3$)$_2$), 27.1 (CH(*C*H$_3$)$_2$), 34.7 (O*C*CH$_3$), 45.7 (*C*H(CH$_3$)$_2$), 71.5 (O*C*Me$_3$), 167.3 ppm (*C*N$_3$); IR (Nujol, KBr): $\tilde{\nu}$ = 1638 (s), 1322 (s), 1257 (s), 1203 (s), 1053 (s), 953 (s), 841(s), 753(m), 687 cm^{-1} (m); elemental analysis calcd (%) forC$_{30}$H$_{73}$N$_6$OSi$_4$Y (735.2): C 49.01, H 9.92, Y 12.09; found: C 48.79; H 9.66; Y 12.37.

*[Nd{(Me$_3$Si)$_2$NC(NiPr)$_2$}$_2$(OtBu)] (**2a**)*: This compound was prepared following the procedure described above for **1a** staring from [{Nd(μ-Cl)[(Me$_3$Si)$_2$NC(N*i*Pr)$_2$}$_2$}$_2$] (2.03 g, 1,35 mmol) in THF (60 mL) and KO*t*Bu (0.31 g, 2.80 mmol) in THF (15 mL). Compound **2a** was isolated as pale blue crystals (1.94 g, 91 %). IR (Nujol, KBr): $\tilde{\nu}$ = 1638 (s), 1603 (m), 1257 (s), 1234 (m), 1049 (s), 957 (s), 922 (m), 838 cm^{-1} (s) cm^{-1}; elemental analysis calcd (%) for C$_{30}$H$_{73}$N$_6$NdOSi$_4$ (790.5): C 45.58, H 9.23, Nd 18.24; found: C 45.19; H 8.91; Nd 18.34.

*[Sm{(Me$_3$Si)$_2$NC(NiPr)$_2$}$_2$(OtBu)] (**3a**)*: This compound was prepared following the procedure described above for **1a** staring from [{Sm(μ-Cl)[(Me$_3$Si)$_2$NC(N*i*Pr)$_2$}$_2$}$_2$] (1.42 g, 0.94 mmol) in THF (60 mL) and KO*t*Bu (0.21 g, 1.90 mmol) in THF (15 mL). Compound **3a** was isolated as pale yellow crystals (1.94 g, 81 %). IR (Nujol, KBr): $\tilde{\nu}$ = 1638 (s), 1252 (s), 1197 (m), 1049 (s), 954 (s), 922 (m), 841 cm^{-1} (s); elemental analysis calcd (%) for C$_{30}$H$_{73}$N$_6$OSi$_4$Sm (796.7): C 45.28, H 9.16, Sm 18.87; found: C 45.66; H 9.41; Sm 18.92.

*[Lu{(Me$_3$Si)$_2$NC(NiPr)$_2$}$_2$(OtBu)] (**4a**)*: This compound was prepared following the procedure described above for **1a** staring from [{(Me$_3$Si)$_2$NC(N*i*Pr)$_2$}$_2$Lu(μ-Cl)Li(thf)$_2$] (0.98 g, 1.01 mmol) in THF (40 mL) and KO*t*Bu (0.11 g, 1.01 mmol) in THF (10 mL). Compound **4a** was isolated as colorless crystals (0.68 g, 82 %). ^{1}H NMR (200 MHz, [D$_6$]benzene): δ = 0.14, 0.24, 0.33 (3 s, together 36 H; NSi(CH_3)$_3$), 1.00, 1.23, 1.27 (d, $^3J_{H\text{-}H}$ = 6.2 Hz, together 24 H; CH(CH_3)$_2$), 1.43, 1.52 (2 s, together 9 H; *t*Bu), 3.75, 3.89, 4.04 ppm (3 sept, $^3J_{H\text{-}H}$ = 6.2 Hz, together 4 H; C*H*(CH$_3$)$_2$); $^{13}C\{^1H\}$ NMR (50 MHz, [D$_6$]benzene): δ = 1.6, 2.1, 2.3 (N(Si*C*H$_3$)$_2$), 22.6, 22.8, 26.8 (CH(*C*H$_3$)$_2$), 31.6, 34.7 (OC*C*H$_3$), 42.5, 45.7, 47.7 (*C*H(CH$_3$)$_2$), 72.4 (O*C*Me$_3$), 167.2 ppm (*C*N$_3$); IR (Nujol, KBr): $\tilde{\nu}$ = 1639 (s), 1252 (s), 1228 (m), 1051 (s), 955 (s), 918 (m), 824 (s), 758 cm^{-1} (m); elemental analysis calcd (%) for C$_{30}$H$_{73}$LuN$_6$OSi$_4$ (821.2): C 43.87, H 8.88, Lu 21.30; found: C 43.50; H 9.00; Lu 21.54.

*[Y{(Me$_3$Si)$_2$NC(NiPr)$_2$}$_2$(OiPr)] (**1b**)*: This compound was prepared following the procedure described above for **1a** staring from [{(Me$_3$Si)$_2$NC(N-*i*Pr)$_2$}$_2$Y(μ-Cl)Li(thf)$_2$] (1.05 g, 1.19 mmol) in THF (30 mL) and NaO*i*Pr (0.11 g, 1.34 mmol) in THF (10 mL). Compound **1b** was isolated as a colorless powder (0.77 g, 90 %). ^{1}H NMR (200 MHz, [D$_6$]benzene): δ = 0.37, 0.44 (2 s, together 36 H; NSi(CH_3)$_3$), 1.31 (d, $^3J_{H\text{-}H}$ = 5.8 Hz, 6 H; OCH(CH_3)$_2$), 1.47 (d, $^3J_{H\text{-}H}$ = 6.3 Hz, 24 H; NCH(CH_3)$_2$), 3.95 (sept, $^3J_{H\text{-}H}$ = 6.3 Hz, 4 H; NC*H*(CH$_3$)$_2$), 4.74 ppm (sept, $^3J_{H\text{-}H}$ = 5.8 Hz, 1 H; OC*H*(CH$_3$)$_2$); $^{13}C\{^1H\}$ NMR (50 MHz, [D$_6$]benzene): δ = 2.6, 3.0 (N(Si*C*H$_3$)$_2$), 27.2 (NCH(*C*H$_3$)$_2$), 29.5 (OCH(*C*H$_3$)$_2$), 45.8 (N*C*H(CH$_3$)$_2$), 64.4 (O*C*H(CH$_3$)$_2$), 166.7 ppm (*C*N$_3$); IR (Nujol, KBr): $\tilde{\nu}$ = 1639 (s), 1601 (w), 1329 (m), 1252 (s), 1229 (m), 1198 (m), 1159 (m), 1144 (m), 1050 (s), 976 (m), 955 (s), 918 (m), 879 (s), 842 (s), 830 (s), 759 (m), 684 (m), 659 (w), 638 (w), 617 (w), 534 cm^{-1} (w); elemental analysis calcd (%) for C$_{29}$H$_{71}$N$_6$OSi$_4$Y (720.5): C 48.33, H 9.85, Y 12.33; found: C 48.02; H 9.76; Y 12.70.

*[Nd{(Me$_3$Si)$_2$NC(NiPr)$_2$}$_2$(OiPr)] (**2b**)*: This compound was prepared following the procedure described above for **1a**, staring from [{Nd(μ-Cl)[(Me$_3$Si)$_2$NC(N*i*Pr)$_2$}$_2$}$_2$] (0.92 g, 0.61 mmol) in THF (15 mL) and NaO*i*Pr (0.11 g, 1.34 mmol) in THF (10 mL). Compound **2b** was isolated as a pale blue powder (0.97 g, 93 %). IR (Nujol, KBr): $\tilde{\nu}$ = 2117 (w), 1638 (s), 1330 (w), 1310 (w), 1262 (m), 1252 (s), 1229 (m), 1181 (w), 1158 (m), 1141 (w), 955 (s), 918 (s), 879 (m), 842 (s), 829 (s), 758 (w), 684 cm^{-1} (w); elemental analysis calcd (%) for C$_{29}$H$_{71}$N$_6$NdOSi$_4$ (775.9): C 44.89, H 9.15, Nd 18.59; found: C 44.42; H 9.50; Nd 18.78.

*[Lu{(Me$_3$Si)$_2$NC(NiPr)$_2$}$_2$(OiPr)] (**4b**)*: This compound was prepared following the procedure described above for **1a** staring from [{(Me$_3$Si)$_2$NC(N-*i*Pr)$_2$}$_2$Lu(μ-Cl)Li(thf)$_2$] (1.26 g, 1.30 mmol) in THF (30 mL) and NaO*i*Pr (0.12 g, 1.46 mmol) in THF (10 mL). Compound **4b** was isolated as a colorless powder (0.97 g, 92 %). ^{1}H NMR (200 MHz, [D$_6$]benzene): δ = 0.38, 0.43 (2 s, together 36 H; NSi(CH_3)$_3$), 1.12, 1.24 (2 d, $^3J_{H\text{-}H}$ = 6.5 Hz, together 6 H; OCH(CH_3)$_2$), 1.41, 1.47 (2 d, $^3J_{H\text{-}H}$ = 6.2 Hz, together 24 H; NCH(CH_3)$_2$, 4.06 (sept, $^3J_{H\text{-}H}$ = 6.2 Hz, 4 H; NC*H*(CH$_3$)$_2$), 4.79 ppm (sept, $^3J_{H\text{-}H}$ = 6.5 Hz, 1 H; OC*H*(CH$_3$)$_2$); $^{13}C\{^1H\}$ NMR (50 MHz, [D$_6$]benzene): δ = 2.7, 3.0 (N(Si*C*H$_3$)$_2$), 26.8, 27.1 (NCH(*C*H$_3$)$_2$), 29.3 (OCH(*C*H$_3$)$_2$), 45.8 (N*C*H(CH$_3$)$_2$), 68.4 (O*C*H(CH$_3$)$_2$), 167.8 ppm (*C*N$_3$); IR (Nujol, KBr): $\tilde{\nu}$ = 1638 (s), 1595 (w), 1308 (m), 1263 (m), 1253 (s), 1229 (m), 1181 (w), 1158 (w), 1075 (w), 1051 (s), 954 (m), 918 (m), 880 (w), 841 (s), 830 (m), 759 (w), 683 cm^{-1} (w); elemental analysis calcd (%) for C$_{29}$H$_{71}$LuN$_6$OSi$_4$ (806.6): C 43.18, H 8.80, Lu 21.69; found: C 43.03; H 9.05; Lu 21.54.

Polymerization of *rac*-lactide: In a typical experiment (Table 2, entry 7), in a glove box, a Schlenk flask was charged with a solution of **2a** (7.0 mg, 8.8 μmol) in toluene (1.0 mL). *rac*-Lactide (0.65 g, 4.40 mmol, 500 equiv) in toluene (3.4 mL) was added rapidly to this solution. The mixture was immediately stirred with a magnetic stir bar at 20 °C for 14 h. After an aliquot of the crude material was sampled by pipette for determining monomer conversion by ^{1}H NMR spectroscopy, the reaction was quenched with acidic methanol (ca. 1.0 mL of a 1.2 M HCl solution in MeOH), and the polymer was precipitated with excess methanol (ca. 100 mL). The polymer was then filtered and dried under vacuum to a constant weight.

Polymerization of *rac*-β-butyrolactone: In a typical experiment (Table 4, entry 5), in a glove box, a Schlenk flask was charged with a solution of **1b** (7.1 mg, 9.8 μmol) in toluene (0.35 mL). β-Butyrolactone (0.17 g, 1.97 mmol, 200 equiv) in toluene (0.30 mL) was added rapidly to this solution. The mixture was immediately stirred with a magnetic stir bar at 20 °C. The reaction was processed and worked-up similarly as described above for lactide polymerization.

X-ray crystallographic studies: The data were collected on a SMART APEX diffractometer (graphite-monochromatic, Mo$_{K\alpha}$ radiation, ω- and θ-scan technique, λ = 0.71073 Å). The structures were solved by direct methods and were refined on F^2 using SHELXTL[30] package. All non-hydrogen atoms were refined anisotropically. The hydrogen atoms in **1c** were found from Fourier syntheses of electron densities and were refined isotropically, whereas H atoms in **1a** and **4a** were placed in calculated positions and were refined in the riding model. SADABS[31] was used to perform area detector scaling and absorption corrections. CCDC-678096 (**1a**), CCDC-678098 (**4a**) and CCDC-678097 (**1c**) contain the supplementary crystallographic data for this paper. These data can be obtained free of charge from The Cambridge Crystallographic Data Centre via www.ccdc.cam.ac.uk/data_request/cif.

Acknowledgements

This work was supported by the Russian Foundation for Basic Research (Grant No. 08-03-00391-à, 07-03-12164-ofi, 06-03-32728-a), Program of the Presidium of the Russian Academy of Science (RAS), and RAS Chemistry and Material Science Division. J.F.C. gratefully thanks the Institut Universitaire de France for a Junior IUF fellowship (2005–2009).

[1] a) S. Mecking, *Angew. Chem.* **2004**, *116*, 1096–1104; *Angew. Chem. Int. Ed.* **2004**, *43*, 1078–1085; b) R. E. Drumright, P. R. Gruber, D. E. Henton, *Adv. Mater.* **2000**, *12*, 1841–1846; c) R. Auras, B. Harte, S. Selke, *Macromol. Biosci.* **2004**, *4*, 835–864; d) C.-S. Ha, J. A. Gardella, *Chem. Rev.* **2005**, *105*, 4205–4232.
[2] a) J. C. Middlenton, A. J. Tipton, *Biomaterials* **2000**, *21*, 2335–2346; b) R. A. Jain, *Biomaterials* **2000**, *21*, 2475–2490.
[3] a) B. J. O'Keefe, M. A. Hillmyer, W. B. Tolman, *J. Chem. Soc. Dalton Trans.* **2001**, 2215–2224; b) O. Dechy-Cabaret, B. Martin-Vaca, D. Bourissou, *Chem. Rev.* **2004**, *104*, 6147–6176.
[4] a) K. B. Aubrecht, K. Chang, M. A. Hillmyer, W. B. Tolman, *J. Polym. Sci. A* **2001**, *39*, 284–293; b) G. R. Giesbrecht, G. D. Whitener, J. Arnold, *J. Chem. Soc. Dalton Trans.* **2001**, 923–927; c) T. M. Ovitt, G. W. Coates, *J. Am. Chem. Soc.* **2002**, *124*, 1316–1326; d) Y. Satoh, N. Ikitake, Y. Nakayama, S. Okuno, H. Yasuda, *J. Organomet. Chem.* **2003**, *667*, 42–52; e) C.-X. Cai, A. Amgoune, C. W. Lehmann, J.-F. Carpentier, *Chem. Commun.* **2004**, 330–331; f) L. Zhang, Z. Shen, C. Yu, L. Fan, *J. Macromol. Sci. A* **2004**, *41*, 927–935; g) H. Ma, J. Okuda, *Macromolecules* **2005**, *38*, 2665–2673; h) F. Bonnet, A. R. Cowley, P. Mountford, *Inorg. Chem.* **2005**, *44*, 9046–9055; i) A. Amgoune, C. M. Thomas, T. Roisnel, J.-F. Carpentier, *Chem. Eur. J.* **2006**, *12*, 169–179; j) A. Amgoune, C. M. Thomas, S. Ilinca, T. Roisnel, J.-F. Carpentier, *Angew. Chem.* **2006**, *118*, 2848–2850; *Angew. Chem. Int. Ed.* **2006**, *45*, 2782–2784; k) I. Westmoreland, J. Arnold, *Dalton Trans.*, **2006**, 4155–4163; l) H. Ma, T. P. Spaniol, J. Okuda, *Angew. Chem.* **2006**, *118*, 7982–7985; *Angew. Chem. Int. Ed.* **2006**, *45*, 7818–7821; m) X. Liu, X. Shang, T. Tang, N. Hu, F. Pei, D. Cui, X. Chen, X. Jing, *Organometallics* **2007**, *26*, 2747–2757; n) P. I. Binda, E. E. Delbridge, *Dalton Trans.* **2007**, 4685–4692; o) J. Wang, T. Cai, Y. Yao, Q. Shen, *Dalton Trans.* **2007**, 5275–5281; p) S. Wang, S. Wang, S. Zhou, G. Yang, W. Luo, N. Hu, Z. Zhou, H.-B. Song, *J. Organomet. Chem.* **2007**, *692*, 2099–2106; q) S. Zhou, S. Wang, E. Sheng, L. Zhang, Z. Yu, X. Xi, G. Chen, W. Luo, Y. Li, *Eur. J. Inorg. Chem.* **2007**, 1519–1528; r) H. Zhou, H. Guo, Y. Yao, L. Zhou, H. Sun, H. Sheng, Y. Zhang, Q. Shen, *Inorg. Chem.* **2007**, *46*, 958–964; s) M. T. Gamer, P. W. Roesky, I. Pallard, M. Le Hellaye, S. M. Guillaume, *Organometallics* **2007**, *26*, 651–657; t) E. E. Delbridge, D. T. Dugah, C. R. Nelson, B. W. Skelton, A. H. White, *Dalton Trans.* **2007**, 143–153.
[5] G. G. Skvortsov, M. V. Yakovenko, P. M. Castro, G. K. Fukin, A. V. Cherkasov, J.-F. Carpentier, A. A. Trifonov, *Eur. J. Inorg. Chem.* **2007**, 3260–3267.
[6] M. H. Chisholm, E. E. Delbridge, *New J. Chem.* **2003**, *27*, 1177–1183.
[7] A. A. Trifonov, G. G. Skvortsov, D. M. Lyubov, G. K. Fukin, E. A. Fedorova, M. N. Bochkarev, *Rus. Chem. Bull. Int. Ed.* **2005**, *54*, 2511–2518.
[8] A. A. Trifonov, E. A. Fedorova, G. K. Fukin, M. N. Bochkarev, *Eur. J. Inorg. Chem.* **2004**, 4396–4401.
[9] Y. Yao, Y. Luo, J. Chen, Z. Zhang, Y. Zhang, Q. Shen, *J. Organomet. Chem.* **2003**, *679*, 229–237.
[10] a) A. A. Trifonov, D. M. Lyubov, E. A. Fedorova, G. K. Fukin, H. Schumann, S. Mühle, M. Hummert, M. N. Bochkarev, *Eur. J. Inorg. Chem.* **2006**, 747–756; b) A. A. Trifonov, G. G. Skvortsov, D. M. Lyubov, N. A. Skorodumova, G. K. Fukin, E. V. Baranov, V. N. Glushakova, *Chem. Eur. J.* **2006**, *12*, 747–756.
[11] W. J. Evans, T. J. Boyle, J. W. Ziller, *Organometallics* **1993**, *12*, 3998–4009.
[12] Effective ionic radii for eight-coordinate metal centers: Nd^{3+} 1.109 Å; Sm^{3+} 1.079 Å; Y^{3+} 1.019 Å; Lu^{3+} 0,977 Å; R. D. Shannon, *Acta Crystallogr. Sect. A* **1976**, *32*, 751–767.
[13] These complexes also slowly decompose in the solid state at room temperature over weeks, as indicated by the appearance of a strong absorption band in the IR spectra characteristic for C≡N bonds.
[14] F. Feil, S. Harder, *Eur. J. Inorg. Chem.* **2005**, 4438–4443.
[15] a) K. H. den Haan, J. L. de Boer, J. H. Teuben, A. L. Spek, B. Kojic-Prodic, G. R. Hays, R. Huis, *Organometallics* **1986**, *5*, 1726–1733; b) M. A. Giardello, V. P. Conticello, L. Brard, M. Sabat, A. L. Rheingold, C. L. Stern, T. J. Marks, *J. Am. Chem. Soc.* **1994**, *116*, 10212–10240; c) M. R. Douglass, M. Ogasawara, S. Hong, M. V. Metz, T. J. Marks, *Organometallics* **2002**, *21*, 283–292.
[16] F. A. Allen, O. Konnard, D. G. Watson, L. Brammer, G. Orpen, R. Taylor, *J. Chem. Soc. Perkin Trans. 1* **1987**, 1–19.
[17] A. Amgoune, C. M. Thomas, J.-F. Carpentier, *Macromol. Rapid Commun.* **2007**, *28*, 693–697.
[18] a) K. A. M. Thakur, R. T. Kean, E. S. Hall, J. J. Kolstad, T. A. Lindgren, M. A. Doscotch, J. I. Siepmann, E. J. Munson, *Macromolecules* **1997**, *30*, 2422–2428; b) J. E. Kasperczyk, *Macromolecules* **1995**, *28*, 3937–3939.
[19] B. M. Chamberlain, Y. Sun, J. R. Hagadorn, E. W. Hemmesch, V. G. Young, Jr., M. Pink, M. A. Hillmyer, W. B. Tolman, *Macromolecules* **1999**, *32*, 2400–2402.
[20] M. H. Chisholm, N. W. Eilerts, *Chem. Commun.* **1996**, 853–854.
[21] A. Le Borgne, C. Pluta, N. Spassky, *Macromol. Rapid Commun.* **1994**, *15*, 955–960.
[22] B. M. Chamberlain, M. Cheng, D. R. Moore, E. B. Lobkovsky, T. M. Ovitt, G. W. Coates, *J. Am. Chem. Soc.* **2001**, *123*, 3229–3238.
[23] L. R. Rieth, D. R. Moore, E. B. Lobkovsky, G. W. Coates, *J. Am. Chem. Soc.* **2002**, *124*, 15239–15248.
[24] J. E. Kemnitzer, S. P. McCarthy, R. A. Gross, *Macromolecules* **1993**, *26*, 1221–1229.
[25] Attempts to perform immortal polymerization of BBL with these systems in the presence of free isopropanol were unsuccessful (see Table 4, entry 7).
[26] a) H. R. Kricheldorf, M. Berl, N. Scharnagi, *Macromolecules* **1988**, *21*, 286–293; b) P. Dubois, C. Jacobs, R. Jérôme, P. Teyssié, *Macromolecules* **1991**, *24*, 2266–2270.
[27] M. D. Taylor, C. P. Carter, *J. Inorg. Nucl. Chem.* **1962**, *24*, 387–393.
[28] L. E. Manzer, *Inorg. Chem.* **1978**, *17*, 1552–1558.
[29] a) I. Barakat, P. Dubois, R. Jerome, P. Teyssié, *J. Polym. Sci. A: Polym. Chem.* **1993**, *31*, 505–514; b) H. Ma, J. Okuda, *Macromolecules* **2005**, *38*, 2665–2673.
[30] G. M. Sheldrick, SHELXTL v. 6.12, Structure Determination Software Suite, Bruker AXS, Madison, Wisconsin (USA), **2000**.
[31] G. M. Sheldrick, SADABS v.2.01, Bruker/Siemens Area Detector Absorption Correction Program, Bruker AXS, Madison, Wisconsin (USA), **1998**.

Received: February 15, 2008
Published online: May 19, 2008

